

## **Antimicrobial graft copolymer gels**

HARVEY, Amanda <<http://orcid.org/0000-0003-3720-2602>>, MADSEN, Jeppe, DOUGLAS, C. W. Ian, MACNEIL, Sheila and ARMES, Steven P.

Available from Sheffield Hallam University Research Archive (SHURA) at:

<https://shura.shu.ac.uk/19158/>

---

This document is the Published Version [VoR]

### **Citation:**

HARVEY, Amanda, MADSEN, Jeppe, DOUGLAS, C. W. Ian, MACNEIL, Sheila and ARMES, Steven P. (2016). Antimicrobial graft copolymer gels. *Biomacromolecules*, 17 (8), 2710-2718. [Article]

---

### **Copyright and re-use policy**

See <http://shura.shu.ac.uk/information.html>

## Antimicrobial Graft Copolymer Gels

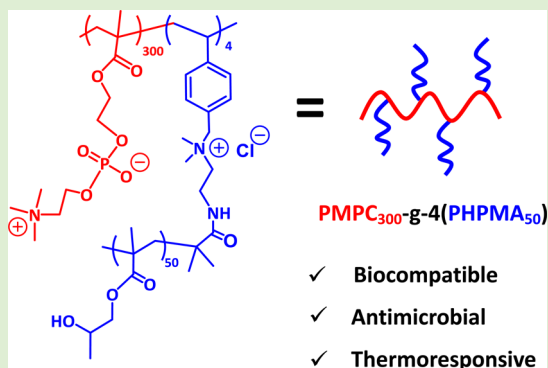
Amanda C. Harvey,<sup>†,‡,§</sup> Jeppe Madsen,<sup>†</sup> C. W. Ian Douglas,<sup>‡</sup> Sheila MacNeil,<sup>§</sup> and Steven P. Armes<sup>\*†</sup>

<sup>†</sup>Department of Chemistry, Dainton Building, University of Sheffield, Brook Hill, Sheffield, South Yorkshire, S3 7HF, United Kingdom

<sup>‡</sup>Unit of Oral and Maxillofacial Pathology, School of Clinical Dentistry, University of Sheffield, Clarendon Crescent, Sheffield, South Yorkshire, S10 2TA, United Kingdom

<sup>§</sup>The Kroto Research Institute, Department of Engineering Materials, University of Sheffield, Broad Lane, Sheffield, South Yorkshire, S3 7HQ, United Kingdom

**ABSTRACT:** In view of the growing worldwide rise in microbial resistance, there is considerable interest in designing new antimicrobial copolymers. The aim of the current study was to investigate the relationship between antimicrobial activity and copolymer composition/architecture to gain a better understanding of their mechanism of action. Specifically, the antibacterial activity of several copolymers based on 2-(methacryloyloxy)ethyl phosphorylcholine [MPC] and 2-hydroxypropyl methacrylate (HPMA) toward *Staphylococcus aureus* was examined. Both block and graft copolymers were synthesized using either atom transfer radical polymerization or reversible addition–fragmentation chain transfer polymerization and characterized via <sup>1</sup>H NMR, gel permeation chromatography, rheology, and surface tensiometry. Antimicrobial activity was assessed using a range of well-known assays, including direct contact, live/dead staining, and the release of lactate dehydrogenase (LDH), while transmission electron microscopy was used to study the morphology of the bacteria before and after the addition of various copolymers. As expected, PMPC homopolymer was biocompatible but possessed no discernible antimicrobial activity. PMPC-based graft copolymers comprising PHPMA side chains (i.e. PMPC-g-PHPMA) significantly reduced both bacterial growth and viability. In contrast, a PMPC–PHPMA diblock copolymer comprising a PMPC stabilizer block and a hydrophobic core-forming PHPMA block did not exhibit any antimicrobial activity, although it did form a biocompatible worm gel. Surface tensiometry studies and LDH release assays suggest that the PMPC-g-PHPMA graft copolymer exhibits surfactant-like activity. Thus, the observed antimicrobial activity is likely to be the result of the weakly hydrophobic PHPMA chains penetrating (and hence rupturing) the bacterial membrane.



### INTRODUCTION

The overuse of antibiotics has led to a worldwide rise in bacterial resistance over several decades with the specter of untreatable infections now looming ever closer.<sup>1–4</sup> Some infections pose particular therapeutic difficulties, which have resulted in various antibiotics becoming ineffective. For example, treatment of low-grade or chronic wound infections has led to nonantibiotic treatments being sought. Among these are the topical application of honey,<sup>5–9</sup> silver,<sup>10–13</sup> and cationic copolymers.<sup>14–22</sup> However, these approaches do not offer a panacea (e.g., silver may compromise wound healing and honey can be difficult to handle), so there is a clinical need to develop new therapies.<sup>23</sup> For this reason, biocompatible materials that are intrinsically antimicrobial and can be easily incorporated into dressings would be useful additions to the therapeutic arsenal for treating infected wounds.

Modern wound dressings employ various polymeric biomaterials,<sup>11,13,24–26</sup> including hydrogels. The latter have the advantages of retaining moisture, exhibiting low cytotoxicity, cooling the wound to reduce pain, being highly absorbent, and, as we describe herein, some may possess inherent

antimicrobial activity.<sup>26–29</sup> Certain biomimetic polymers can mimic the chemical structure of mammalian cell membranes, which make them ideal candidates for in vivo biomedical applications where biocompatibility is of paramount importance.<sup>16,19,26,30,31</sup>

We have previously reported that thermo-responsive PHPMA–PMPC–PHPMA triblock copolymer gelators [where MPC = 2-(methacryloyloxy)ethyl phosphorylcholine and HPMA = 2-hydroxypropyl methacrylate] can serve as biocompatible gelators for novel wound dressings.<sup>31,32</sup> Moreover, these particular copolymer gels exhibited unexpected antimicrobial activity toward *Staphylococcus aureus* and other micro-organisms. In principle, several physicochemical properties of these novel copolymer gels may be important for the observed antimicrobial activity. It was shown that the PHPMA component was essential for this activity but the precise mode of action was unknown. Previously, we reported that a range of

Received: May 25, 2016

Revised: July 4, 2016

Published: July 13, 2016

micro-organisms were killed/inhibited by a PHPMA<sub>88</sub>–PMPC<sub>400</sub>–PHPMA<sub>8</sub> triblock copolymer gelator.<sup>32</sup> In the present study, we examine how the architecture of several types of PHPMA-based copolymers influences antibacterial performance and probe the mechanism of action. To address these two fundamental questions, we chose to focus on a single micro-organism, *S. aureus*.

The aim of the present study is to explore in more detail the relationship between antimicrobial activity and the copolymer composition/architecture of this potentially useful class of biomaterials.

## MATERIALS

2-(Methacryloyloxy)ethyl phosphorylcholine monomer (MPC, 99.9% purity) was donated by Biocompatibles U.K. Ltd. (Farnham, U.K.). 2-Hydroxypropyl methacrylate (HPMA) was donated by GEO Specialty Chemicals (Hythe, U.K.). Bis(2-hydroxyethyl)disulfide (98%), 2-bromoisobutyl bromide (98%), 4-vinylbenzyl chloride, basic alumina (Brockmann I, standard grade, 150 mesh, 58 Å), anhydrous methanol (99.8%), copper chloride (Cu(I)Cl, 99.995%), copper bromide (Cu(I)Br, 99.9%), and 2,2'-bipyridine (bpy, 99%), triethylamine (99%), cetyltrimethylammonium bromide (CTAB), and cresyl violet acetate (70%) were purchased from Sigma-Aldrich U.K. (Dorset, U.K.). All these chemicals were used as received, except for triethylamine, which was refluxed over potassium hydroxide and kept sealed over potassium hydroxide. The silica gel 60 (0.063–0.200 μm) used to remove the spent ATRP catalyst was purchased from E. Merck (Darmstadt, Germany). Propan-1,3-diol was purchased from Hopkins and Williams (London, U.K.). All solvents were HPLC-grade and purchased from Fisher Scientific (Loughborough, U.K.). Deionized water was used in all experiments.

Three strains of *S. aureus* were employed in this study: NCTC 6571 (Oxford), S235, and L9879. The former is a laboratory standard strain used in sensitivity assays, strain S235 is a clinical isolate, and strain L9879 is relatively hydrophilic compared with the other two strains. The latter was included because it was hypothesized that this feature might influence its interaction with the copolymer gels. The culture medium, Brain Heart Infusion (BHI) broth, and agar were purchased from Oxoid (Basingstoke, U.K.). Live/dead staining was performed using propidium iodide (PI) and Syto 9, which were purchased from Invitrogen (Paisley, U.K.). Dulbecco's modified Eagle's medium (DMEM) and EDTA were purchased from Sigma-Aldrich (Poole, Dorset, U.K.). Fetal calf serum (FCS) was purchased from Labtech (Ringmer, U.K.). Glutamine, penicillin, and streptomycin were purchased from Gibco (Paisley, U.K.). MTT (3-(4,5-dimethylthiazol-2-yl)-2,5-diphenyl tetrazolium bromide) powder, MTS 3-(4,5-dimethylthiazol-2-yl)-5-(3-carboxymethoxyphenyl)-2-(4-sulfophenyl)-2H-tetrazolium, and Lysostaphin were purchased from Sigma-Aldrich (Dorset, U.K.). Isopropanol and 7-hydroxy-3H-phenoxazin-3-one 10-oxide (Resazurin–Alamar Blue) were purchased from Fisher Scientific (Leicestershire, U.K.). Trypsin was purchased from Difico Laboratories (Detroit, MI, U.S.A.). An LDH-Cytotoxicity Assay Kit II was purchased from Abcam (Abcam, U.K.).

**Homopolymerization of HPMA by ATRP.** PHPMA homopolymer was prepared via ATRP with a target degree of polymerization (DP) of 50. More specifically, HPMA monomer (20.0 g, 0.139 mol), 2-(dimethylamino)ethyl-2-bromoisobutyrylamide initiator (prepared as described previously;<sup>33</sup> 1.09 g, 4.63 mmol), bpy (1.44 g, 9.26 mmol), and a 90:10 v/v IPA/H<sub>2</sub>O mixture (20 mL) were placed in a round-bottomed flask. This was placed on ice and degassed by purging with nitrogen through a needle for 30 min. Then Cu(I)Cl (0.463 g, 4.63 mmol) was added quickly to the stirred solution under a positive nitrogen pressure and the reaction solution was heated to 50 °C in an oil bath for 24 h. The reaction solution was exposed to air, cooled, and diluted with methanol. This quenching protocol resulted in a change in color from dark brown to blue/green, which indicated aerial oxidation of the catalyst. The solution was passed through a short silica column and washed repeatedly with methanol to remove the spent

Cu(I)Cl. Solvent evaporation using a rotary evaporator and drying on a vacuum line overnight afforded a tertiary amine-functionalized PHPMA homopolymer as a white powder.

**Quaternization of PHPMA Macromonomer.** PHPMA homopolymer (23.9 g, 5.54 mmol) was dissolved in methanol (12.6 mL) to give a 25% w/v solution. To this solution, 4-vinylbenzyl chloride (4-VBC; 2.54 g, 16.6 mmol; VBC/PHPMA molar ratio = 3.0) was added and the reaction mixture was stirred at 20 °C for 48 h. Excess 4-VBC was then removed by precipitation three times into cyclohexane (700 mL). Residual solvent was removed by rotary evaporation and the resulting solid was recovered and dried on a vacuum line overnight. The resulting purified styrene-functionalized PHPMA macromonomer was characterized by <sup>1</sup>H NMR spectroscopy. The mean degree of quaternization was calculated by comparing the aromatic styrene end-group signals at δ 7.55–7.70 to the two azamethylene protons assigned to the tertiary amine end-group of the PHPMA chain at δ 3.61–3.77.<sup>25</sup>

**Cresyl Violet-Labeled PHPMA Macromonomer by ATRP.** Fluorescently labeled macromonomers were prepared by the addition of cresyl violet (CV; λ<sub>em</sub> = 600 nm) in its acetate salt form. This dye functions as a chain transfer agent that reacts irreversibly with the propagating PHPMA radicals, thus adding the fluorescent label at the end of the propagating chain-end. Care was taken to minimize exposure to light during this synthesis. HPMA (20.0 g, 0.138 mol), 2-(dimethylamino)ethyl-2-bromoisobutyrylamide initiator (0.658 g, 2.77 mmol), and cresyl violet acetate (0.223 g, 2.77 mmol) were dissolved in a 90:10 IPA/H<sub>2</sub>O v/v mixture (20 mL) and the resulting solution was cooled on ice, degassed, and kept under a nitrogen atmosphere for 40 min. Cu(I)Cl (0.275 g, 2.77 mmol) and bpy (0.866 g, 5.55 mmol) were then added and the solution was heated to 50 °C in an oil bath and stirred for 24 h, at which point samples were taken for <sup>1</sup>H NMR and dimethylformamide gel permeation chromatography (GPC). The resulting CV-terminated PHPMA homopolymer precursor was dissolved in methanol and passed through a silica column to remove the spent catalyst as well as any free CV dye. Excess solvent was removed via rotary evaporation to afford a purple solid.

**Synthesis of 1,3-Bis(2-(thiobenzoylthio)prop-2-yl)benzene [TBTPB].** TBTPB was synthesized according to previously reported methods.<sup>34</sup> Dithiobenzoic acid (DTBA) was synthesized as described previously.<sup>35</sup> DTBA (48.0 g, 0.311 mol, 1.0 equiv), 1,3-diisopropenylbenzene (49.0 g, 0.311 mol, 1.0 equiv), *p*-toluenesulfonic acid (2.00 g, 2.0% w/v), and CCl<sub>4</sub> (160 mL) was mixed under a nitrogen atmosphere and refluxed for 18 h at 75 °C in an oil bath. After cooling to room temperature, a saturated solution of NaHCO<sub>3</sub> (200 mL) was added. After extraction with dichloromethane (2 × 100 mL) the organic layers were combined, washed with a saturated sodium chloride solution (400 mL) and dried over MgSO<sub>4</sub> before being evaporated under reduced pressure by rotary evaporation to afford a dark purple oil/solid. The crude product was further purified by column chromatography on a 20 g scale using neutral silica as a stationary phase and a mixed eluent comprising ethyl acetate and petroleum ether using a gradient of ethyl acetate ranging from 5 to 10%. This procedure was repeated twice to afford sufficient purity as judged by TLC (yield: 86 g, 87%).

**Preparation of PMPC<sub>300</sub> Homopolymer by RAFT Polymerization.** TBTPB (0.0485 g, 0.104 mmol, 1.0 equiv) and MPC monomer (5.00 g, 31.2 mmol, 300.0 equiv) were dissolved in ethanol (3.37 mL) to produce a 40% w/v solution in a round-bottom flask. The flask was then placed on ice and purged with nitrogen for 15 min. Once degassed, the flask was removed from the ice, ACVA (0.0073 g, 26.0 μmol, 0.25 equiv) was added, and the solution was degassed further for 5 min. The reaction solution was heated to 80 °C in an oil bath. Samples were removed regularly for <sup>1</sup>H NMR and GPC analysis. At high monomer conversion, the solution was cooled and exposed to air. The crude homopolymer was diluted with methanol, dialyzed (dialysis membrane molecular weight cut-off = 1000 Da) first against methanol and then against deionized water. An aqueous solution of the purified PMPC homopolymer was then frozen in a round-bottomed flask using a liquid nitrogen bath before being freeze-dried overnight. PMPC<sub>300</sub> was recovered as a light pink solid (yield: 4.9 g, 97%).

**PMPC<sub>300</sub>-g-4(PHPMA<sub>50</sub>) Graft Copolymer by RAFT Polymerization.** PMPC<sub>300</sub>-g-4(PHPMA<sub>50</sub>) graft copolymers were prepared via a one-pot synthesis using a bifunctional RAFT agent (TBTPB). The copolymer was targeted with an overall DP of 300 MPC units plus four PHPMA<sub>50</sub> macromonomer units per backbone: PHPMA<sub>50</sub> macromonomer (3.26 g, 0.452 mmol, 4.0 equiv) was dissolved in ethanol (19 mL) by the aid of ultrasonication. This solution was added to a round-bottomed flask containing TBTPB (0.0308 g,  $1.13 \times 10^{-4}$  mol, 1.0 equiv) and MPC monomer (10.0 g,  $3.39 \times 10^{-2}$  mol, 300.0 equiv) to afford a 40% w/v solution. The flask was then placed on ice and purged with nitrogen for 30 min. Once degassed, the flask was removed from the ice and ACVA (0.0079 g,  $2.82 \times 10^{-5}$  mol, 0.25 equiv) was added and the flask was degassed further for 5 min. The reaction solution was heated to 80 °C using an oil bath. Samples were extracted over time for <sup>1</sup>H NMR and GPC analysis. After 48 h, <sup>1</sup>H NMR showed very little residual monomer. At this point, the solution was cooled and exposed to air. The copolymer was diluted with methanol, dialyzed using a dialysis membrane (MWCO = 1000 Da) first against methanol and then deionized water. The purified copolymer was then frozen in a round-bottom flask using liquid nitrogen before being freeze-dried overnight. PMPC<sub>300</sub>-g-4(PHPMA<sub>50</sub>) was recovered as a light pink solid (12.2 g, 92% yield). A similar protocol was used to prepare an equivalent graft copolymer using the CV-labeled PHPMA macromonomer described above. This additional sample is denoted as "PMPC<sub>300</sub>-g-4(cvPHPMA<sub>50</sub>)".

**PMPC<sub>25</sub>-PHPMA<sub>275</sub> Diblock Copolymer Worms.** The PMPC<sub>25</sub>-PHPMA<sub>275</sub> worms were synthesized as described previously.<sup>36</sup>

**PHPMA<sub>88</sub>-PMPC<sub>400</sub>-PHPMA<sub>88</sub> Triblock Copolymer.** The PHPMA<sub>88</sub>-PMPC<sub>400</sub>-PHPMA<sub>88</sub> triblock copolymer was synthesized using a bifunctional disulfide-based ATRP initiator, as described previously.<sup>31</sup>

**<sup>1</sup>H NMR Spectroscopy.** <sup>1</sup>H NMR spectra were recorded in CD<sub>3</sub>OD at 20 °C using a Bruker DPX-400 NMR spectrometer. Spectra were analyzed using SpinWorks3 software (2010 Kirk Marat, University of Manitoba, Canada).

**Molecular Weight Determination.** Molecular weight distributions were assessed at 40 °C using a Hewlett-Packard HP1090 liquid chromatograph pump in combination with two Polymer Laboratories PL Gel 5 μm Mixed-C (7.5 × 300 mm) columns in series with a guard column connected to a Gilson Model 131 refractive index detector. The eluent was a 3:1 v/v chloroform/methanol mixture containing 2.0 mM LiBr at a flow rate of 1.0 mL min<sup>-1</sup>. Calibration was achieved using a series of near-monodisperse poly(methyl methacrylate) [PMMA] standards. Copolymers were dissolved in this mixed eluent at a concentration of 5 mg dm<sup>-3</sup> and filtered before injection. Data analyses were conducted using Cirrus™ GPC Software supplied by Polymer Laboratories.<sup>37</sup>

**Gel Rheology Studies.** These measurements were conducted as described previously.<sup>37</sup> Copolymer dispersions of varying concentration were prepared by addition of aqueous phosphate buffered saline (PBS) solution at 0 °C followed by vigorous shaking and storage at 4 °C overnight prior to analysis. A Rheometric Scientific SR-5000 rheometer, equipped with a cone-plate geometry (40.0 mm, 0.05 radians) and a Peltier unit for temperature control, was used to perform the oscillatory temperature sweeps. This was conducted at a frequency of 1.0 rad s<sup>-1</sup>, an applied stress of 0.50 Pa, and a heating rate of 3 °C min<sup>-1</sup> from 5 to 50 °C.

**Surface Tensiometry.** All copolymers were dissolved in deionized water at concentrations ranging from  $5.0 \times 10^{-4}$  % to 1.0% w/v and stirred overnight to ensure full dissolution. These were compared with control solutions of cetyltrimmonium bromide (CTAB), a well-known cationic surfactant, over the same concentration range. Surface tensions were determined using a Lauda TD3 surface tensiometer at various temperatures controlled by a water bath. The Du Nouy method was utilized, which required a Pt ring (circumference = 4 cm). Prior to each measurement, the Pt ring was washed in ethanol and water after burning off any organic residue. The ring was then lowered into each aqueous solution until the ring was located approximately 5 mm below the liquid surface. The surface tension was determined as

the minimum normal detachment force required to remove the Pt ring from the water surface. Measurements were repeated six times per sample and the results were averaged.

**Cell Culture Studies.** Human skin was obtained from patients undergoing breast reductions and abdominoplasty elective surgical procedures who gave informed consent for skin not required for their treatment to be used on an anonymous basis for research as part of a Human Research Tissue Bank [HTA] license number 12179. Fibroblasts were isolated from skin according to the methods described by Ghosh et al.<sup>38</sup> Fibroblasts were isolated and cultured in Dulbecco's Modified Eagle's Medium (DMEM), supplemented with 10% v/v fetal calf serum (FCS), 2.0 mmol dm<sup>-3</sup> glutamine, 0.625 mg dm<sup>-3</sup> amphotericin B, 100 mg dm<sup>-3</sup> streptomycin and 100 IU/mL penicillin.<sup>7</sup> Cell viability and metabolic activity were assessed using Alamar Blue. Monolayers were washed three times in PBS and incubated with 1.0 g dm<sup>-3</sup> Alamar Blue solutions in a 24-well plate for 60 min at 37 °C with 5% CO<sub>2</sub>. The eluted dye was transferred to a 96-well plate. The absorbance of each solution was determined at 540 nm using a spectrophotometer.

**Antimicrobial Assays.** *Staphylococcus aureus* strains NCTC 6571 (Oxford), S235, and L9879 were cultured on brain heart infusion (BHI) agar or in BHI broth at 37 °C for 16 h, as required.

**Direct Contact Assay.** This involved placing copolymer onto bacterial films on BHI agar. A single colony of *S. aureus* was suspended in 10 mL of sterile PBS and evenly distributed over the surface of BHI agar plates with a swab. Dilutions of appropriate copolymer preparations (5 to 20% w/v of PMPC-based statistical, block or graft copolymers, respectively) were then pipetted in 10 μL aliquots directly onto the surface of the bacterial films at 4 °C before incubating at 37 °C overnight. The resulting culture was assessed for its effect on bacterial growth.

**Live/Dead Staining.** Fluorescently labeled PMPC<sub>300</sub>-g-4(PHPMA<sub>50</sub>) graft copolymer was dissolved in PBS to produce a 12% w/w gel. Aliquots of *S. aureus* suspension ( $1 \times 10^6$  CFU) were pelleted via centrifugation, resuspended in cold copolymer solution and incubated overnight at 37 °C. Samples were then cooled on ice for 10 min to convert the thermoresponsive copolymer gel into a liquid. Bacteria were then separated from the copolymer by centrifugation at 13 000 rpm at 4 °C for 4 min. The bacteria were incubated with the fluorescent dyes Syto 9 [1.5 μL of 3.34 mM solution in DMSO] and PI [1.5 μL of 20 mM solution in DMSO] for 30 min before washing excess dye from the bacteria three times using PBS. The bacteria were then examined using a fluorescence ZEISS LSM 510 M confocal microscope with excitation wavelengths of 488 and 543 nm. Emission spectra were recorded between 515 and 615 nm. The PI dye can only traverse damaged membranes while the Syto 9 dye diffuses into all cells, thus differentiating dead (red) cells from live (green) cells. Confocal images were analyzed using LSM Image Browser software (Carl Zeiss).

**Lactate Dehydrogenase (LDH) Assay.** Bacterial viability following exposure to copolymer was also assessed by monitoring the release of lactate dehydrogenase (LDH). *S. aureus* S235 (150 μL; OD = 1.50,  $1 \times 10^8$ ) was incubated overnight either with a 12% w/v PMPC<sub>300</sub>-g-4(PHPMA<sub>50</sub>) aqueous dispersion or with an equal volume (150 μL 1% w/v 1 mg/mL) of a positive control of glycyglycine metalloendopeptidase, (lysostaphin). Samples were incubated 37 °C for 18 h, cooled on ice for 10 min to convert the copolymer gel into a free-flowing liquid, and centrifuged at 13 000 rpm at 4 °C for 4 min to sediment the bacteria. Aliquots of copolymer supernatant (50 μL) were removed and assayed for LDH activity using a commercial LDH-Cytotoxicity Assay Kit II (Abcam Ltd.) by recording the optical density using a plate reader operating at 495 nm.

**Transmission Electron Microscopy (TEM).** Bacteria were exposed to a 12% w/v aqueous PMPC<sub>300</sub>-g-4(PHPMA<sub>50</sub>) copolymer gel and then isolated using the protocol described above. Copper TEM grids (Agar Scientific, U.K.) were surface-coated with a thin film of amorphous carbon and then plasma glow-discharged for 30 s to create a hydrophilic surface. Droplets (5.0 μL) of the bacteria suspensions obtained from the LDH assay described above were adsorbed onto the freshly glow-discharged grids, air-dried, and then blotted with filter

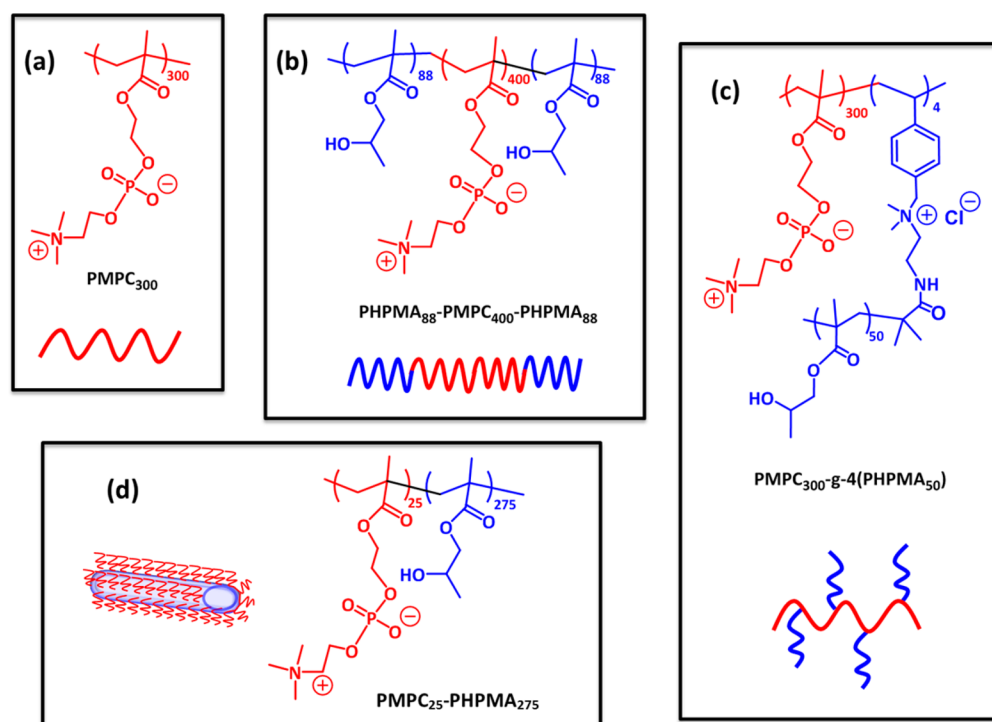


**Figure 1.** Various copolymer compositions and architectures examined in this study: (a) PMPC<sub>300</sub> homopolymer control; (b) PHPMA<sub>88</sub>–PMPC<sub>400</sub>–PHPMA<sub>88</sub> triblock copolymer; (c) PMPC<sub>300</sub>-g-4(PHPMA<sub>50</sub>); (d) PMPC<sub>25</sub>–PHPMA<sub>275</sub> worms (control).

**Table 1. Summary of Target Copolymer Compositions, Monomer Conversions, Molecular Weight Data, and Biological Activities for the PMPC Homopolymer, the PMPC<sub>25</sub>–PHPMA<sub>275</sub> Diblock Copolymer, PHPMA<sub>88</sub>–PMPC<sub>400</sub>–PHPMA<sub>88</sub> Triblock Copolymer, and the PMPC<sub>300</sub>-g-4(PHPMA<sub>50</sub>) Graft Copolymer Examined in This Study**

copolymer composition	synthesis method	conversion [ <sup>1</sup> H NMR]	$M_w/M_n^a$	$M_n$ [kg/mol]	gel?	biocompatible?	antimicrobial?
PMPC <sub>300</sub>	RAFT	98%	1.21	40.8	no	yes	no
PMPC <sub>25</sub> –PHPMA <sub>275</sub>	RAFT	99%	1.29	72.0	yes	yes	no
PHPMA <sub>88</sub> –PMPC <sub>400</sub> –PHPMA <sub>88</sub>	ATRP	96%	1.35	89.5	yes	yes	yes
PMPC <sub>300</sub> -g-4(PHPMA <sub>50</sub> )	RAFT	96%	1.33	78.6	yes	yes	yes

<sup>a</sup>GPC analysis using a refractive index detector, a 3:1 CHCl<sub>3</sub>/methanol mixed eluent containing 2.0 mM LiCl, and a series of near-monodisperse poly(methyl methacrylate) (PMMA) calibration standards.

paper to remove excess solution. Grids were rinsed with distilled water, stained with uranyl formate (0.75% w/v) for 20 s, and then carefully blotted to remove excess stain. After washing twice with deionized water and drying under high vacuum, imaging was performed at 100 kV using a Phillips CM100 instrument equipped with a Gatan 1 k CCD camera.

## RESULTS AND DISCUSSION

In order to prepare well-defined PMPC<sub>300</sub>-g-4(PHPMA<sub>50</sub>) graft copolymers, near-monodisperse PHPMA macromonomers were first prepared using atom transfer radical polymerization (ATRP) via a two-step synthetic route previously reported by Armes and co-workers.<sup>39,40</sup> First, HPMA was polymerized using a tertiary amine-functionalized ATRP initiator in methanol at 20 °C to produce a PHPMA homopolymer precursor. Then the terminal tertiary amine group was quaternized using excess 4-vinylbenzyl chloride (4-VBC) in methanol at 20 °C to afford the desired near-monodisperse styrene-functionalized PHPMA macromonomer.<sup>33</sup> Optionally, cresyl violet was incorporated into the PHPMA macromonomers as a fluorescent end-group to enable fluorescent visualization when investigating biological activity. Cresyl violet acetate acts as a spin trap and reacts irreversibly with the

propagating PHPMA radicals, thus adding the desired fluorescent label to the end of the chain. Finally, the PHPMA macromonomer was statistically copolymerized with MPC to produce the final PMPC-g-4(PHPMA<sub>50</sub>) graft copolymer using RAFT polymerization via a grafting-through process. The target PHPMA content was four macromonomer chains per copolymer backbone for these model graft copolymers, which is twice the number of PHPMA blocks per copolymer chain compared to the PHPMA–PMPC–PHPMA triblock copolymers reported earlier.<sup>31,32,41</sup> This graft copolymer composition was selected in order to produce an efficient gelator.

The synthesis of the PMPC<sub>25</sub>–PHPMA<sub>275</sub> diblock copolymer worms is based on the principle of polymerization-induced self-assembly (PISA), as reported by Sugihara et al.<sup>36</sup> First, a well-defined PMPC<sub>25</sub> macromolecular chain transfer agent (macro-CTA) was prepared by conventional RAFT solution polymerization of MPC in water. Then this macro-CTA was used for the RAFT aqueous dispersion polymerization of HPMA at 70 °C. To ensure reproducible targeting of the worm phase, Sugihara et al. found it necessary to use a relatively short PMPC block and also had to construct a detailed phase diagram.<sup>36</sup> The resulting PMPC<sub>25</sub>–PHPMA<sub>275</sub> diblock copolymer worms were used as a control in the present study and

formed soft free-standing aqueous gels at a copolymer concentration of around 10% w/w at 20 °C.<sup>36</sup>

MPC was selected as a comonomer for this study because of its well-known biocompatibility and well-controlled (co)-polymerization using living radical polymerization techniques such as ATRP or RAFT polymerization.<sup>42–53</sup> A schematic representation of the various copolymers used in this study is depicted in Figure 1.

Table 1 summarizes the (co)polymers prepared in this study. As expected, the PMPC homopolymer prepared via RAFT polymerization did not form an aqueous gel. Another important reference material for the present study was PMPC<sub>25</sub>–PHPMA<sub>275</sub>, which self-assembles to form highly anisotropic worm-like particles in aqueous solution.<sup>36</sup> Multiple interworm contacts are formed, leading to the formation of a soft free-standing gel. Although relatively short, the highly hydrophilic PMPC block acts as an effective steric stabilizer for the worms, while the relatively long, weakly hydrophobic PHPMA block forms the worm cores. Thus, this copolymer was expected to be biocompatible but to possess little or no antimicrobial activity. In contrast, the final two entries shown in Table 1 are PMPC<sub>300</sub>-g-4(PHPMA<sub>50</sub>) graft copolymers prepared via RAFT statistical copolymerization of MPC with the PHPMA<sub>50</sub> macromonomer. These copolymers comprise a relatively long PMPC-based backbone (target mean degree of polymerization = 300) with a statistical distribution of approximately four pendant PHPMA<sub>50</sub> chains. This architecture can be compared to the PHPMA–PMPC–PHPMA triblock copolymers previously reported by Madsen and co-workers.<sup>31</sup> In both cases, near-molecular dissolution can be achieved in cold aqueous solution (below 5 °C), with self-assembly occurring on warming to ambient temperature as the PHPMA blocks become increasingly hydrophobic.

Relatively low polymer polydispersities were obtained for PMPC homopolymer, the PMPC<sub>25</sub>–PHPMA<sub>275</sub> diblock copolymer, and the PMPC-based graft copolymers, as expected for such pseudoliving polymerizations.<sup>54,55</sup> The cresyl violet-labeled PHPMA<sub>50</sub> macromonomer was successfully incorporated into the graft copolymer chains. However, regardless of whether a labeled or an unlabeled macromonomer was used, the statistical copolymerization of MPC with PHPMA<sub>50</sub> macromonomer was significantly slower than the homopolymerization of MPC under the same conditions (see Figure 2).

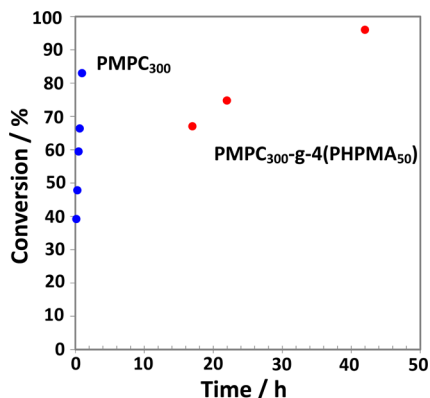


**Figure 2.** Conversion versus time curves obtained from <sup>1</sup>H NMR studies of the synthesis of PMPC<sub>300</sub>-g-4(PHPMA<sub>50</sub>) at 70 °C prepared using the TBTPB RAFT agent at 40% w/v solids (red circles) and PMPC<sub>300</sub> homopolymer under similar conditions (blue circles).

More specifically, more than 40 h were required to achieve high monomer conversions (at least 96%) when the PHPMA<sub>50</sub> macromonomer was used, compared to less than 3 h without this comonomer. Further work is required to understand these perplexing observations, which we are currently unable to explain; it is particularly surprising given that there are relatively few macromonomer chains per graft copolymer chain (MPC/styrene molar ratio = 75).

The thermoresponsive PMPC<sub>300</sub>-g-4(PHPMA<sub>50</sub>) graft copolymer gels were characterized by rheological measurements using a cone-and-plate geometry setup. A temperature sweep was performed for each copolymer between 2 and 40 °C in which an oscillatory stress of 0.50 Pa was applied at a frequency of 1.0 rad s<sup>-1</sup> using a heating ramp rate of 3 °C min<sup>-1</sup>. The storage (*G'*) and loss (*G''*) moduli exhibit differing temperature-dependent behavior and the point at which *G''* crosses *G'* indicates the critical gelation temperature (CGT), see Figure 3.

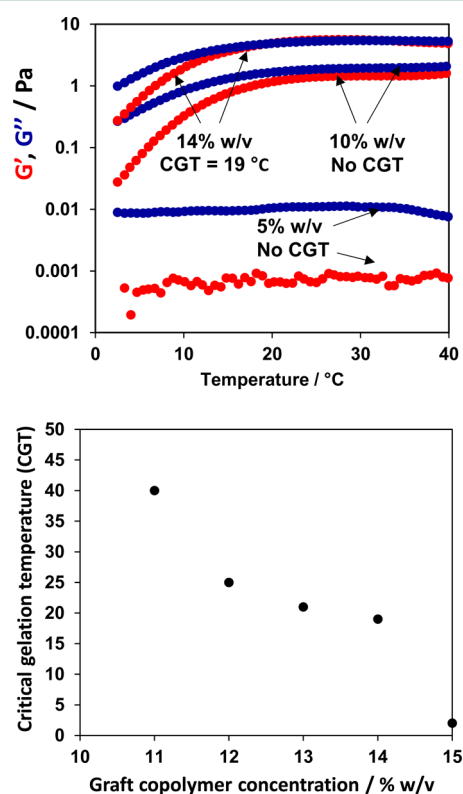


**Figure 3.** Temperature-dependent rheology data for a PMPC<sub>300</sub>-g-4(PHPMA<sub>50</sub>) graft copolymer gel prepared via ATRP: (a) *G'* and *G''* moduli determined for 10 and 13% w/v aqueous graft copolymer gels from 2 to 50 °C at a heating rate of 3 °C min<sup>-1</sup>; (b) CGT values determined for 10–15% w/v aqueous graft copolymer gels. Note that increasing the copolymer concentration significantly reduces the CGT.

This parameter is rather sensitive to the copolymer concentration: a CGT of approximately 39 °C is observed for an 11% w/w graft copolymer gel but this is reduced to less than 5 °C for a 15% w/w graft copolymer gel (see Figure 3B). Thus, the CGT can be readily adjusted over a wide range of physiologically relevant temperatures simply by varying the copolymer concentration. A similar inverse relationship between CGT and copolymer concentration was reported by Madsen et al. for the analogous PHPMA–PMPC–PHPMA triblock copolymer gels.<sup>31</sup>

Copolymer gel biocompatibility was evaluated over 24 h by placing copolymer gels in direct contact with a monolayer of human dermal fibroblast (HDF) cells. No discernible detrimental effect on cell viability was observed, see Figure 4. These results were not unexpected, given that similar findings had been reported previously by Bertal et al. for PHPMA–PMPC–PHPMA triblock copolymer gels.<sup>32</sup>

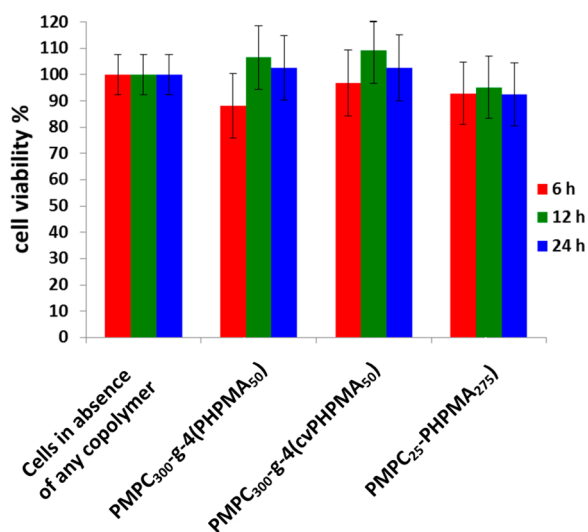


**Figure 4.** Cell viabilities for various copolymers determined over 24 h using HDF cells measured with Alamar Blue. Copolymers were utilized at their optimum concentrations in each case: the graft copolymers were used at 12.5% w/v, while PMPC<sub>25</sub>–HPMA<sub>275</sub> worm gels were employed at 25% w/v. Copolymer gels were applied directly on top of HDF monolayers in a thin layer (200  $\mu$ L per 24-well plate) which was supplemented with 200 mL 10% DMEM solution to ensure that the cells did not dry out. Error bars = standard deviation, data representative of  $n = 3$ .

To assess the antimicrobial activity of each copolymer, direct contact assays were performed using each of the three strains of *S. aureus*. First, various copolymer hydrogel dispersions/solutions were placed on top of films of S235, L9879, and Oxford on agar gel. Typical results are shown in Figure 5. The nongelling aqueous copolymer solution of 5% w/v PMPC<sub>300</sub>-g-4(PHPMA<sub>50</sub>) did not inhibit bacterial growth but using the same copolymer in the form of a 10% w/w free-standing gel reduced bacterial growth, see Figure 5E, 5F. Similar results were obtained for all three strains. This antimicrobial performance is comparable to that observed for a 15% w/w PHPMA<sub>80</sub>–PMPC<sub>400</sub>–PHPMA<sub>80</sub> triblock copolymer gel prepared by Madsen et al. (see Figure 5D),<sup>31</sup> which suggests that the graft copolymer architecture may be more effective than a triblock copolymer architecture. Importantly, the PMPC<sub>25</sub>–PHPMA<sub>275</sub> diblock copolymer worm gel did not exhibit any discernible antimicrobial activity, even at a copolymer concentration of 25% w/w (see Figure 5B). This indicates that gelation alone is not sufficient to suppress bacterial growth. Moreover, appropriate spatial location of the PHPMA chains is clearly critical for antimicrobial activity. This interpretation is supported by previous reported findings by Bertal and co-workers, who found that planar surfaces coated with PHPMA brushes exhibited antimicrobial activity, whereas those coated with PMPC brushes did not.<sup>32</sup>

Confocal microscopy studies were undertaken using a well-documented live/dead assay based on the combination of two

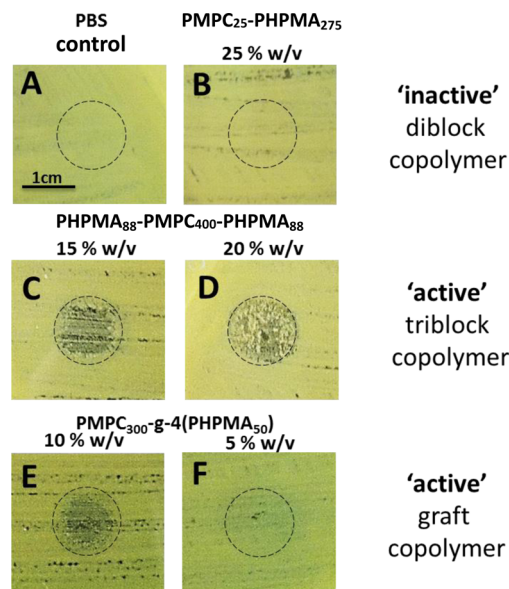


**Figure 5.** “Drop-on” assay used to assess the antimicrobial activity of various copolymers toward *S. aureus* (S235). Reduced growth within the droplet area (see dotted line) indicates an inhibitory effect toward *S. aureus*. (a) PBS control; (b) 25% w/v PMPC<sub>25</sub>–PHPMA<sub>275</sub> diblock copolymer worm gel;<sup>16</sup> (c,d) PHPMA<sub>88</sub>–PMPC<sub>400</sub>–PHPMA<sub>88</sub> triblock copolymer gel<sup>13,14</sup> utilized at 15% w/v and 20% w/v, respectively; (e,f) PMPC<sub>300</sub>-g-4(PHPMA<sub>50</sub>) graft copolymer gel utilized at 10% w/v and 5% w/v, respectively. Copolymers are designated as “active” or “inactive” according to whether an antimicrobial effect is observed toward *S. aureus* growth with similar results being obtained for all three strains investigated in this work. Black dotted line indicates the droplet area, reduction of yellow bacteria growth is indicated by the dark background. Images representative of  $n = 3$ .

fluorescent dye probes, SYTO 9 and propidium iodide (PI).<sup>56</sup> The former dye stains live bacteria green, whereas the latter dye stains dead bacteria red. *S. aureus* was mixed with a 12% w/v cresyl violet-labeled graft copolymer gel [denoted PMPC<sub>300</sub>-g-4(cvPHPMA<sub>50</sub>)] for 16 h at 37 °C, after which each gel was cooled to produce a free-flowing liquid. This enabled the bacteria to be sedimented via centrifugation and hence isolated for examination by confocal microscopy. Representative images are shown in Figure 6, together with a positive control comprising heat-treated dead bacteria and also untreated live bacteria as a negative control. The fluorescent cresyl violet label signal (purple) is colocalized within the bacteria, suggesting ingress of the copolymer chains within the micro-organism. As expected, all heat-treated bacteria appeared red (dead) and all live bacteria appeared green. Following exposure to the 12% w/v solution of PMPC<sub>300</sub>-g-4(cvPHPMA<sub>50</sub>) graft copolymer, most of the bacteria appeared dead with only a small number of viable bacteria being observed. This provides the direct experimental evidence that such PMPC<sub>300</sub>-g-4(PHPMA<sub>50</sub>) graft copolymer gels are actually antibacterial, as opposed to being merely bacteriostatic.

To further examine the mechanism of antimicrobial activity, release of a cytoplasmic enzyme (lactate dehydrogenase, or LDH) from the bacteria was assessed using a commercial enzyme assay, see Figure 7. The positive control involved exposure of bacteria to lysostaphin while the negative control was simply a suspension of cells in PBS alone. Treating *S. aureus* (S235) with either graft copolymer or lysostaphin

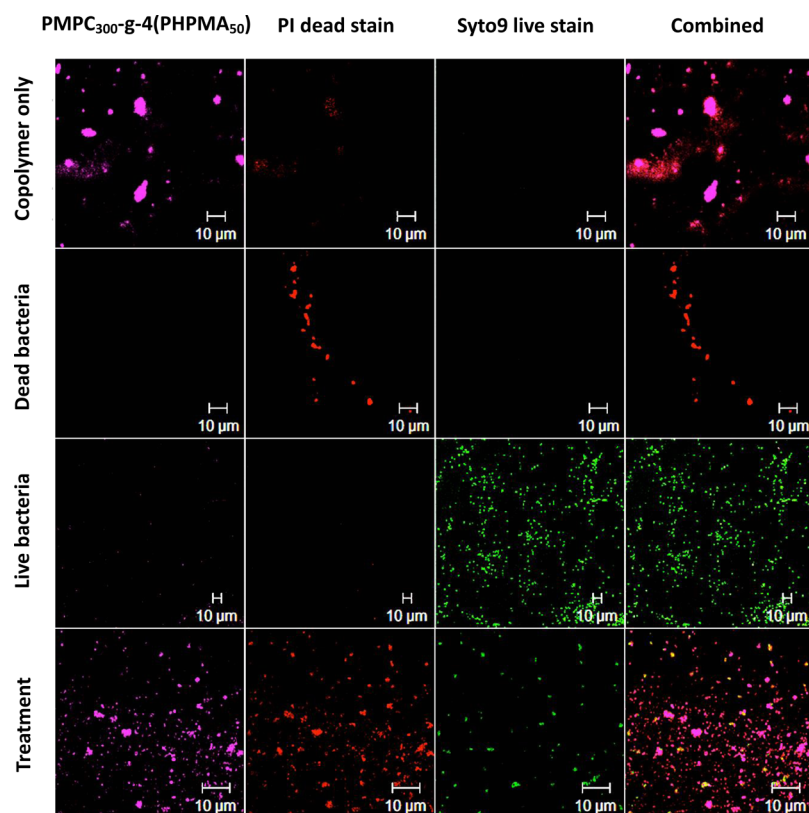


**Figure 6.** Confocal laser scanning microscopy studies illustrating the live/dead assay for *S. aureus* [NCTC 6571 (Oxford) strain] after treatment with a 12.5% w/v PMPC<sub>300</sub>-g-4(PHPMA<sub>50</sub>) graft copolymer gel. Copolymer-only (purple channel, top row of panels) shows isolation of the CV signal. Heat-treated dead bacteria (red channel) are shown as a control in the second row of panels. Live bacteria are shown as a control in the red channel (third row of panels). The fourth row of panels show copolymer-treated bacteria; overlays indicate colocalization of the copolymer with the dead bacteria.

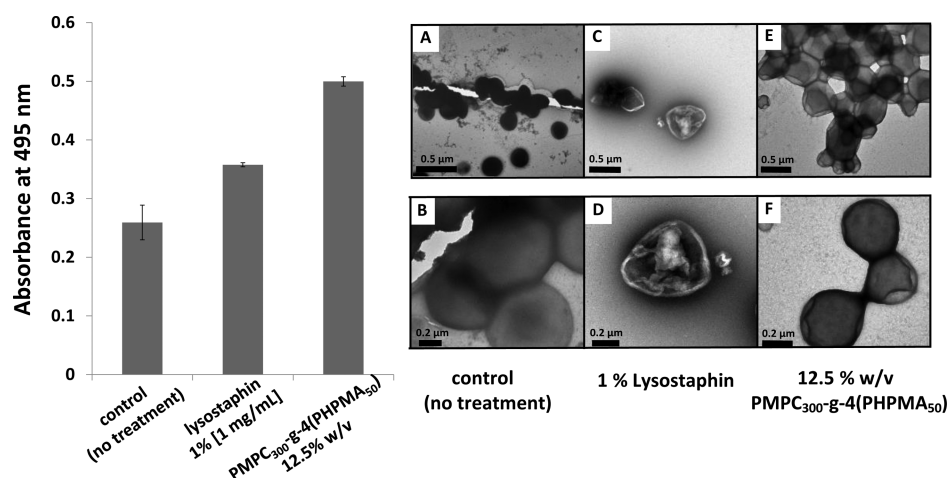


**Figure 7.** Exposure to a 10% w/v PMPC<sub>300</sub>-g-4(PHPMA<sub>50</sub>) graft copolymer gel causes bacterial membrane damage to *S. aureus* (S235 strain). LDH release from this micro-organism is observed in the presence of both lysostaphin (positive control) and the graft copolymer, compared to a negative control (PBS alone). TEM images indicate that compared to a control sample (A,B), the bacterial membrane is compromised for *S. aureus* treated with either lysostaphin (C,D) or PMPC<sub>300</sub>-g-4(PHPMA<sub>50</sub>) (E,F). In addition, there is some evidence for the aggregation of bacteria when treated with the PMPC<sub>300</sub>-g-4(PHPMA<sub>50</sub>) copolymer.

resulted in a significant increase in the concentration of extracellular LDH, with the copolymer producing the greater response. Thus, this assay provides good evidence that the graft copolymer causes significant damage to the bacterial membrane. Presumably, the weakly hydrophobic PHPMA<sub>50</sub> chains penetrate the cell membrane, causing its rupture. This bactericidal mechanism is not possible for the PMPC<sub>25</sub>-

PHPMA<sub>275</sub> diblock copolymer worm gel because in this case its relatively long PHPMA chains form the worm cores and hence cannot interact with the bacteria.

TEM was used to examine whether there were any changes in bacteria morphology upon treatment with copolymer gels. Untreated *S. aureus* cells exhibit a well-defined spherical morphology, see Figure 7A, 7B. In contrast, *S. aureus* cells

treated with the lytic endopeptidase, lysostaphin, appeared as “empty cell ghosts”, see Figure 7C, 7D.<sup>57,58</sup> In contrast, bacteria treated with 12.5% PMPC<sub>300</sub>-g-4(PHPMA<sub>50</sub>) are somewhat deformed with apparent membrane shrinkage from the cell wall, see Figure 7E, 7F. In addition, there is some evidence for bacteria aggregation in the presence of the PMPC<sub>300</sub>-g-4(PHPMA<sub>50</sub>) copolymer.

In principle, the antibacterial mechanism for the PMPC<sub>300</sub>-g-4(PHPMA<sub>50</sub>) copolymer may be similar to that of cationic surfactants. To examine this hypothesis, the concentration dependence of the surface tension of dilute aqueous copolymer solutions was determined and compared with that of cetyltrimethylammonium bromide (CTAB).<sup>59</sup> Such cationic surfactants are known to kill micro-organisms by rupturing bacterial cell membranes.<sup>19,21</sup> Pure water has a surface tension of 72 mN m<sup>-1</sup> at 25 °C. As expected, CTAB had a relatively low limiting surface tension of 36 mN m<sup>-1</sup> at 1.0% w/w concentration, see Figure 8. The PMPC<sub>300</sub>-g-4(PHPMA<sub>50</sub>)

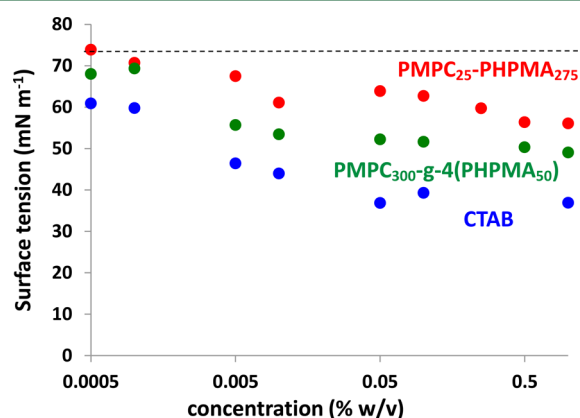


**Figure 8.** Surface tension versus copolymer concentration curves for PMPC<sub>300</sub>-g-4(PHPMA<sub>50</sub>) graft copolymer, PMPC<sub>25</sub>-PHPMA<sub>275</sub> worms and a cationic surfactant (cetyltrimethylammonium bromide, CTAB) at 4 °C.

copolymer exhibited a limiting surface tension of 49 mN m<sup>-1</sup> at 1.0% w/w concentration, which is comparable to that obtained for other non-ionic water-soluble polymers such as poly(*N*-vinylpyrrolidone). This surface activity is attributed to adsorption of the hydrophobic PHPMA chains at the air–water interface because PMPC homopolymer causes little or no lowering of the aqueous surface tension (see Figure 8). Moreover, the PMPC<sub>25</sub>-PHPMA<sub>275</sub> diblock copolymer worms also exhibited much lower surface activity than that of the PMPC<sub>300</sub>-g-4(PHPMA<sub>50</sub>) graft copolymer because in the former case the PHPMA blocks are located within the worm cores and hence are not available for adsorption at the air–water interface. Thus, there is an obvious correlation between surface activity and antimicrobial activity, which is consistent with the proposed mechanism of action for the new PMPC<sub>300</sub>-g-4(PHPMA<sub>50</sub>) graft copolymers described herein.

The present study has confirmed that the *spatial location* of the PHPMA chains plays a critical role in determining antimicrobial activity toward *S. aureus*. The relatively long PHPMA blocks present in the PMPC<sub>25</sub>-PHPMA<sub>275</sub> diblock copolymer self-assemble in aqueous solution to form the cores of sterically stabilized worms, which leads to no detectable antimicrobial activity. In contrast, the relatively short PHPMA blocks present in the PHPMA–PMPC–PHPMA triblock

copolymers previously reported by Madsen et al. and in the PMPC<sub>300</sub>-g-4(PHPMA<sub>50</sub>) graft copolymers described herein are sufficiently hydrophobic and surface-active to rupture bacterial membranes. There is some evidence that the new graft copolymer architecture is more potent than the triblock copolymer architecture reported previously. In summary, we have established that gelation alone is not sufficient to kill *S. aureus* but it is not yet clear whether gelation enhances antimicrobial activity. Finally, one reviewer of this manuscript has suggested that the microstructure of these graft copolymers could also affect their antimicrobial performance. This interesting hypothesis also clearly warrants further work.

## CONCLUSIONS

Inhibition of bacterial growth can be achieved using the new PMPC-g-PHPMA graft copolymer gel described herein. Moreover, there is some evidence that this new copolymer architecture may be more effective than the PHPMA–PMPC–PHPMA triblock copolymer gels described previously. Importantly, new control experiments conducted using biocompatible PMPC<sub>25</sub>-b-PHPMA<sub>275</sub> diblock copolymer worm gels confirm that no antibacterial activity is observed in this case. Thus, the spatial location of the PHPMA chains is clearly critical for the observation of antimicrobial activity and gelation alone is not sufficient to inhibit bacterial growth. A confocal microscopy-based live/dead assay provides evidence that PMPC<sub>300</sub>-g-4(PHPMA<sub>50</sub>) graft copolymer gel does indeed kill micro-organisms, rather than merely retarding their growth. It is postulated that the weakly hydrophobic PHPMA chains penetrate the bacterial membrane and hence induce rupture, as indicated by the in situ release of LDH. TEM studies provide evidence for bacteria aggregation, while confocal microscopy studies conducted using a fluorescently labeled graft copolymer confirm its interaction with the micro-organism. It is emphasized that this new antibacterial graft copolymer gel exhibits relatively low cytotoxicity toward mammalian cells. Given its thermoreversible gelation behavior, it may also offer some potential as an inherently antibacterial smart wound dressing.

## AUTHOR INFORMATION

### Corresponding Author

\*E-mail: [s.p.arnes@shef.ac.uk](mailto:s.p.arnes@shef.ac.uk)

### Notes

The authors declare no competing financial interest.

## ACKNOWLEDGMENTS

We thank BBSRC for funding a PhD studentship for A.C.H. and EPSRC for a Platform grant for S.P.A. (EP/J007846/1). Dr. N. J. Warren is thanked for the synthesis of the PBBIB initiator and Dr. S. Sugihara is acknowledged for the synthesis of the PMPC<sub>25</sub>-PHPMA<sub>275</sub> worm gel control. Dr L. P. D. Ratcliffe is thanked for TEM analysis and Dr. J. Rosselgong and Dr P. C. Yang are acknowledged for their advice regarding copolymer syntheses. We also thank Mr J. Z. Heath for assistance with some of the antimicrobial assays and Dr N. Brown for her assistance with the confocal microscopy studies.

## REFERENCES

- Andersson, D. I.; Hughes, D. *Nat. Rev. Microbiol.* **2010**, *8*, 260–271.

- (2) Gbaguidi-Haore, H.; Dumartin, C.; L'hériteau, F.; Péfau, M.; Hocquet, D.; Rogues, A.-M.; Bertrand, X. *J. Antimicrob. Chemother.* **2013**, *68*, 461–470.
- (3) Livermore, D. M. *Clin. Infect. Dis.* **2003**, *36*, S11–23.
- (4) Rodier, G. *WHO Reg. Comm. Eur.* **2011**, *61*, 1–13.
- (5) Lusby, P. J. *WOCN* **2002**, *29*, 295–300.
- (6) Al-Waili, N.; Salom, K.; Al-Ghamdi, A. A. *Sci. World J.* **2011**, *11*, 766–787.
- (7) Cooper, R. a.; Molan, P. C.; Harding, K. G. *J. R. Soc. Med.* **1999**, *92*, 283–285.
- (8) Lay-flurrie, K. *Br. J. Nurs.* **2008**, *17*, S30–S36.
- (9) Visavadia, B. G.; Honeysett, J.; Danford, M. H. *Br. J. Oral Maxillofac. Surg.* **2008**, *46*, 55–56.
- (10) Storm-Versloot, M. N.; Vos, C. G.; Ubbink, D. T.; Vermeulen, H. *Cochrane database Syst. Rev.* **2010**, *3*, 1–108.
- (11) Bergin, S.; Wraight, P. *Cochrane Database Syst. Rev.* **2011**, *2*, 1–24.
- (12) Warriner, R.; Burrell, R. *Adv. Skin Wound Care* **2005**, *18*, 2–12.
- (13) Vermeulen, H.; Van Hattem, J.; Storm-Versloot, M.; Ubbink, D.; Westerbos, S. *Cochrane database Syst. Rev.* **2007**, *1*, 1–43.
- (14) Sambhy, V.; Peterson, B. R.; Sen, A. *Angew. Chem., Int. Ed.* **2008**, *47*, 1250–1254.
- (15) Muñoz-Bonilla, A.; Fernández-García, M. *Prog. Polym. Sci.* **2012**, *37*, 281–339.
- (16) Siedenbiedel, F.; Tiller, J. C. *Polymers* **2012**, *4*, 46–71.
- (17) Palermo, E. F.; Kuroda, K. *Appl. Microbiol. Biotechnol.* **2010**, *87*, 1605–1615.
- (18) Nederberg, F.; Zhang, Y.; Tan, J. P. K.; Xu, K.; Wang, H.; Yang, C.; Gao, S.; Guo, X. D.; Fukushima, K.; Li, L.; Hedrick, J. L.; Yang, Y.-Y. *Nat. Chem.* **2011**, *3*, 409–414.
- (19) Lenoir, S.; Pagnouille, C.; Detrembleur, C.; Galleni, M.; Jérôme, R. *J. Polym. Sci., Part A: Polym. Chem.* **2006**, *44*, 1214–1224.
- (20) Hoque, J.; Akkapeddi, P.; Yarlagadda, V.; Uppu, D. S. S. M.; Kumar, P.; Haldar, J. *Langmuir* **2012**, *28*, 12225–12234.
- (21) Murata, H.; Koepsel, R. R.; Matyjaszewski, K.; Russell, A. J. *Biomaterials* **2007**, *28*, 4870–4879.
- (22) Colomer, A.; Pinazo, A.; Manresa, M. A.; Vinardell, M. P.; Mitjans, M.; Infante, M. R.; Pérez, L. *J. Med. Chem.* **2011**, *54*, 989–1002.
- (23) Muñoz-Bonilla, A.; Fernández-García, M. *Eur. Polym. J.* **2015**, *65*, 46–62.
- (24) Boateng, J. S.; Matthews, K. H.; Stevens, H. N. E.; Eccleston, G. M. *J. Pharm. Sci.* **2008**, *97*, 2892–2923.
- (25) Rizzi, S. C.; Upton, Z.; Bott, K.; Dargaville, T. R. *Expert Rev. Med. Devices* **2010**, *7*, 143–154.
- (26) Overstreet, D. J.; Huynh, R.; Jarbo, K.; McLemore, R. Y.; Vernon, B. L. *J. Biomed. Mater. Res., Part A* **2013**, *101A*, 1437–1446.
- (27) Moody, A. *Br. J. Community Nurs.* **2006**, *11*, S12–S17.
- (28) Li, Y.; Fukushima, K.; Coady, D. J.; Engler, A. C.; Liu, S.; Huang, Y.; Cho, J. S.; Guo, Y.; Miller, L. S.; Tan, J. P. K.; Ee, P. L. R.; Fan, W.; Yang, Y. Y.; Hedrick, J. L. *Angew. Chem.* **2013**, *125*, 702–706.
- (29) Zhou, J.; Loftus, A. L.; Mulley, G.; Jenkins, A.; Toby, A. *J. Am. Chem. Soc.* **2010**, *132*, 6566–6570.
- (30) Massignani, M.; LoPresti, C.; Blanazs, A.; Madsen, J.; Armes, S. P.; Lewis, A. L.; Battaglia, G. *Small* **2009**, *5*, 2424–2432.
- (31) Madsen, J.; Armes, S. P.; Bertal, K.; Lomas, H.; Macneil, S.; Lewis, A. L. *Biomacromolecules* **2008**, *9*, 2265–2275.
- (32) Bertal, K.; Shepherd, J.; Douglas, C. W. I.; Madsen, J.; Morse, A.; Edmondson, S.; Armes, S. P.; Lewis, A.; Macneil, S. *J. Mater. Sci.* **2009**, *44*, 6233–6246.
- (33) Thompson, K. L.; Bannister, I.; Armes, S. P.; Lewis, A. L. *Langmuir* **2010**, *26*, 4693–4702.
- (34) Guice, K. B.; Marrou, S. R.; Gondi, S. R.; Sumerlin, B. S.; Loo, Y.-L. *Macromolecules* **2008**, *41*, 4390–4397.
- (35) Perrier, S.; Barner-Kowollik, C.; Quinn, J. F.; Vana, P.; Davis, T. P. *Macromolecules* **2002**, *35*, 8300–8306.
- (36) Sugihara, S.; Blanazs, A.; Armes, S. P.; Ryan, A. J.; Lewis, A. L. *J. Am. Chem. Soc.* **2011**, *133*, 15707–15713.
- (37) Madsen, J.; Armes, S. P.; Bertal, K.; Macneil, S.; Lewis, A. L. *Biomacromolecules* **2009**, *10*, 1875–1887.
- (38) Ghosh, M. M.; Boyce, S.; Layton, C.; Freedlander, E.; Neil, S. M. *Ann. Plast. Surg.* **1997**, *39*, 390–404.
- (39) Yang, P.; Armes, S. P. *Langmuir* **2012**, *28*, 13189–13200.
- (40) Dupin, D.; Thompson, K. L.; Armes, S. P. *Soft Matter* **2011**, *7*, 6797–6800.
- (41) Madsen, J.; Armes, S. P.; Lewis, A. L. *Macromolecules* **2006**, *39*, 7455–7457.
- (42) Bhuchar, N.; Sunasee, R.; Ishihara, K.; Thundat, T.; Narain, R. *Bioconjugate Chem.* **2012**, *23*, 75–83.
- (43) Du, J.; Tang, Y.; Lewis, A. L.; Armes, S. P. *J. Am. Chem. Soc.* **2005**, *127*, 17982–17983.
- (44) Feng, W.; Zhu, S.; Ishihara, K.; Brash, J. L. *Langmuir* **2005**, *21*, 5980–5987.
- (45) Ishihara, K.; Ueda, T.; Nakabayashi, N. *Polym. J.* **1990**, *22*, 355–360.
- (46) Iwasaki, Y.; Ishihara, K. *Anal. Bioanal. Chem.* **2005**, *381*, 534–546.
- (47) Lewis, A. L. *Colloids Surf., B* **2000**, *18*, 261–275.
- (48) Li, C.; Madsen, J.; Armes, S. P.; Lewis, A. L. *Angew. Chem., Int. Ed.* **2006**, *45*, 3510–3513.
- (49) Lobb, E. J.; Ma, L.; Billingham, N. C.; Armes, S. P.; Lewis, A. L.; Park, F. B.; Lane, W. *J. Am. Chem. Soc.* **2001**, *123*, 7913–7914.
- (50) Lomas, H.; Canton, I.; MacNeil, S.; Du, J.; Armes, S. P.; Ryan, A. J.; Lewis, A. L.; Battaglia, G. *Adv. Mater.* **2007**, *19*, 4238–4243.
- (51) Ma, Y.; Tang, Y.; Billingham, N. C.; Armes, S. P.; Lewis, A. L.; Lloyd, A. W.; Salvage, J. P. *Macromolecules* **2003**, *36*, 3475–3484.
- (52) Yu, B.; Lowe, A. B.; Ishihara, K. *Biomacromolecules* **2009**, *10*, 950–958.
- (53) Yusa, S.-I.; Fukuda, K.; Yamamoto, T.; Ishihara, K.; Morishima, Y. *Biomacromolecules* **2005**, *6*, 663–670.
- (54) Chiefari, J.; Chong, Y. K. B.; Ercole, F.; Krstina, J.; Jeffery, J.; Le, T. P. T.; Mayadunne, R. T. A.; Meijs, G. F.; Moad, C. L.; Moad, G.; Rizzardo, E.; Thang, S. H.; South, C. *Macromolecules* **1998**, *31*, 5559–5562.
- (55) Wang, J.; Matyjaszewski, K. *J. Am. Chem. Soc.* **1995**, *117*, 5614–5615.
- (56) Stocks, S. M. *Cytometry* **2004**, *61A*, 189–195.
- (57) Haslberger, A. G.; Kohl, G.; Felnerova, D.; Mayr, U. B.; Fu, S. J. *Biotechnol.* **2000**, *83*, 57–66.
- (58) Bexfield, A.; Bond, A. E.; Roberts, E. C.; Dudley, E.; Nigam, Y.; Thomas, S.; Newton, R. P.; Ratcliffe, N. a. *Microbes Infect.* **2008**, *10*, 325–333.
- (59) Kuperkar, K.; Prasad, K.; Abezgauz, L.; Bahadur, P. *J. Surfactants Deterg.* **2010**, *13*, 293–303.